

# Surfaces with prescribed mean curvature in $\mathbb{H}^2 \times \mathbb{R}$

Antonio Bueno<sup>†</sup>, Irene Ortiz<sup>‡</sup>

<sup>†</sup>Departamento de Ciencias e Informática, Centro Universitario de la Defensa de San Javier, E-30729 Santiago de la Ribera, Spain.

*E-mail address:* antonio.bueno@ cud.upct.es

<sup>‡</sup>Departamento de Ciencias e Informática, Centro Universitario de la Defensa de San Javier, E-30729 Santiago de la Ribera, Spain.

*E-mail address:* irene.ortiz@ cud.upct.es

## Abstract

In this paper we study rotational surfaces in the space  $\mathbb{H}^2 \times \mathbb{R}$  whose mean curvature is given as a prescribed function of their angle function. These surfaces generalize, among others, the ones of constant mean curvature and the translating solitons of the mean curvature flow. Using a phase plane analysis we construct entire rotational graphs, catenoid-type surfaces, and exhibit a classification result when the prescribed function is linear.

## 1 Introduction

Let us consider a function  $\mathcal{H} \in C^1(\mathbb{S}^2)$ . An oriented surface  $\Sigma$  immersed into  $\mathbb{R}^3$  is said to be a surface with *prescribed mean curvature*  $\mathcal{H}$  if its mean curvature function  $H_\Sigma$  satisfies

$$H_\Sigma(p) = \mathcal{H}(N_p) \quad (1.1)$$

for every point  $p \in \Sigma$ , where  $N$  denotes the *Gauss map* of  $\Sigma$ . For short, we say that  $\Sigma$  is an  $\mathcal{H}$ -*surface*. Let us observe that when the function  $\mathcal{H}$  is chosen as a constant  $H_0$ , the surfaces defined by Equation (1.1) are just the surfaces with constant mean curvature (CMC) equal to  $H_0$ .

The definition of this class of immersed surfaces has its origins on the famous Christoffel and Minkowski problems for ovaloids [Chr, Min]. The existence of prescribed mean curvature ovaloids was studied, among others, by Alexandrov, Pogorelov and Guan-Guan [Ale, Pog, GuGu], while the uniqueness in the Hopf sense has been recently achieved by Gálvez and Mira [GaMi1]. In this fashion, the first author jointly with Gálvez and Mira started to develop the *global theory of surfaces with prescribed mean curvature in  $\mathbb{R}^3$* , taking as motivation the fruitful theory of CMC surfaces, see [BGM1, BGM2]. The first author also proved the existence and uniqueness to the Björling problem [Bue3] and obtained half space theorems for  $\mathcal{H}$ -surfaces [Bue4].

A relevant case of  $\mathcal{H}$ -surfaces appears when the function  $\mathcal{H}$  depends only on the height of the sphere, i.e., if there exists a one dimensional function  $\mathfrak{h} \in C^1([-1, 1])$  such that  $\mathcal{H}(x) = \mathfrak{h}(\langle x, e_3 \rangle)$  for every  $x \in \mathbb{S}^2$ . In this case,  $\mathcal{H}$  is called *rotationally symmetric* and Equation (1.1) reads as

$$H_\Sigma(p) = \mathfrak{h}(\langle N_p, e_3 \rangle) = \mathfrak{h}(\nu(p)), \quad (1.2)$$

---

*Mathematics Subject Classification:* 53A10, 53C42, 34C05, 34C40.

*Keywords:* Prescribed mean curvature surface, non-linear autonomous system, phase plane analysis.

for every point  $p \in \Sigma$ , where  $\nu(p) := \langle N_p, e_3 \rangle$  is the so-called *angle function* of  $\Sigma$ . In this setting, the authors have obtained a classification result for rotational  $\mathcal{H}$ -hypersurfaces in  $\mathbb{R}^{n+1}$  satisfying (1.2), whose prescribed function  $\mathfrak{h}$  is *linear*, i.e.  $\mathfrak{h}(y) = ay + \lambda$ ,  $a, \lambda \in \mathbb{R}$ , see [BuOr].

Note that for defining Equation (1.2) we only need to measure the projection of a unit normal vector field onto a Killing vector field. Consequently, surfaces obeying (1.2) can be also defined in the product spaces  $\mathbb{M}^2 \times \mathbb{R}$ , where  $\mathbb{M}^2$  is a complete surface, as follows:

**Definition 1.1** *Let  $\mathfrak{h}$  be a  $C^1$  function on  $[-1, 1]$ . An oriented surface  $\Sigma$  immersed in  $\mathbb{M}^2 \times \mathbb{R}$  has prescribed mean curvature  $\mathfrak{h}$  if its mean curvature function  $H_\Sigma$  satisfies*

$$H_\Sigma(p) = \mathfrak{h}(\langle \eta_p, \partial_z \rangle), \quad (1.3)$$

for every point  $p \in \Sigma$ , where  $\eta$  is a unit normal vector field on  $\Sigma$  and  $\partial_z$  is the unit vertical Killing vector field on  $\mathbb{M}^2 \times \mathbb{R}$ .

Again, note that  $\nu(p) := \langle \eta_p, \partial_z \rangle$  is the angle function of  $\Sigma$ . In analogy with the Euclidean case, we will simply say that  $\Sigma$  is an  $\mathfrak{h}$ -surface.

Observe that if  $\mathfrak{h} \equiv H_0 \in \mathbb{R}$ , we recover the theory of CMC surfaces in  $\mathbb{M}^2 \times \mathbb{R}$ , which experienced an extraordinary development since Abresch and Rosenberg [AbRo] defined a *holomorphic quadratic differential* on them, that vanishes on rotational examples. Also, if  $\mathfrak{h}(y) = y$ , the  $\mathfrak{h}$ -surfaces arising are the translating solitons of the mean curvature flow, see [Bue1, Bue2, LiMa]. For a general function  $\mathfrak{h} \in C^1([-1, 1])$  under necessary and sufficient hypothesis, the first author obtained a Delaunay-type classification result in  $\mathbb{M}^2 \times \mathbb{R}$  [Bue5], and a structure-type result for properly embedded  $\mathfrak{h}$ -surfaces in  $\mathbb{H}^2 \times \mathbb{R}$  [Bue6].

Inspired by the fruitful theory of  $\mathcal{H}$ -surfaces in  $\mathbb{R}^3$ , the purpose of this paper is to further investigate the theory of surfaces satisfying (1.3) in the product space  $\mathbb{H}^2 \times \mathbb{R}$ . The  $\mathfrak{h}$ -surfaces studied in this paper are motivated by the examples arising in the theory of minimal surfaces and translating solitons in both  $\mathbb{R}^3$  and  $\mathbb{H}^2 \times \mathbb{R}$ , and by  $\mathcal{H}$ -hypersurfaces in  $\mathbb{R}^{n+1}$  where  $\mathcal{H} \in C^1(\mathbb{S}^n)$  is a linear function.

The rest of the introduction is devoted to detail the organization of the paper and highlight some of the main results.

In Section 2 we deduce the formulae that the profile curve of a rotational  $\mathfrak{h}$ -surface in  $\mathbb{H}^2 \times \mathbb{R}$  satisfy. The resulting ODE will be treated as a non-linear autonomous system, and its qualitative study will be carried out by developing a phase plane analysis. From the previous work [BGM2] we compile the main features of the phase plane adapted to the space  $\mathbb{H}^2 \times \mathbb{R}$ . In Corollary 2.5 we prove the existence of two unique rotational  $\mathfrak{h}$ -surfaces,  $\Sigma_+$  and  $\Sigma_-$ , intersecting orthogonally the axis of rotation with unit normal  $\pm \partial_z$ , respectively.

In Section 3 we prove in Proposition 3.1 the existence of entire, strictly convex  $\mathfrak{h}$ -graphs, called  $\mathfrak{h}$ -bowls in analogy with translating solitons. In Proposition 3.2 we construct properly embedded  $\mathfrak{h}$ -annuli, called  $\mathfrak{h}$ -catenoids for their resemblance to the usual minimal catenoids in  $\mathbb{R}^3$  and  $\mathbb{H}^2 \times \mathbb{R}$ .

In Section 4 we focus on  $\mathfrak{h}_\lambda$ -surfaces, which are defined to be those whose prescribed function is linear, i.e.  $\mathfrak{h}_\lambda(y) := ay + \lambda$ ,  $a, \lambda \in \mathbb{R}$ . The relevance of  $\mathfrak{h}_\lambda$ -surfaces is that they satisfy certain

characterizations that are closely related with the theory of manifolds with density. For instance,  $\mathfrak{h}_\lambda$ -surfaces have *constant weighted mean curvature* equal to  $\lambda$  with respect to the density  $e^\phi$ , where  $\phi(x) = a\langle x, \partial_z \rangle$ ,  $\forall x \in \mathbb{H}^2 \times \mathbb{R}$ . In particular, if  $\lambda = 0$  we recover the fact that translating solitons are weighted minimal as pointed out by Ilmanen [Ilm]. Also,  $\mathfrak{h}_\lambda$ -surfaces are critical points for the weighted area functional, under compactly supported variations preserving the weighted volume (see [BCMR] and [BuOr]).

In this section we obtain our two main results in which we achieve a classification of complete rotational  $\mathfrak{h}_\lambda$ -surfaces in  $\mathbb{H}^2 \times \mathbb{R}$ . First, we prove that we can reduce to study the case  $\mathfrak{h}_\lambda(y) = y + \lambda$ ,  $\lambda > 0$ . If such  $\mathfrak{h}_\lambda$ -surfaces intersect the axis of rotation we get:

**Theorem 1.2** *Let be  $\Sigma_+$  and  $\Sigma_-$  the complete, rotational  $\mathfrak{h}_\lambda$ -surfaces in  $\mathbb{H}^2 \times \mathbb{R}$  intersecting the rotation axis with upwards and downwards orientation respectively. Then:*

1. For  $\lambda > 1/2$ ,  $\Sigma_+$  is properly embedded, simply connected and converges to the flat CMC cylinder  $C_\lambda$  of radius  $\arg \tanh\left(\frac{1}{2\lambda}\right)$ . Moreover:
  - 1.1. If  $\lambda > \sqrt{2}/2$ ,  $\Sigma_+$  intersects  $C_\lambda$  infinitely many times.
  - 1.2. If  $\lambda = \sqrt{2}/2$ ,  $\Sigma_+$  intersects  $C_\lambda$  a finite number of times and is a graph outside a compact set.
  - 1.3. If  $\lambda < \sqrt{2}/2$ ,  $\Sigma_+$  is a strictly convex graph over the disk in  $\mathbb{H}^2$  of radius  $\arg \tanh\left(\frac{1}{2\lambda}\right)$ .
2. For  $\lambda \leq 1/2$ ,  $\Sigma_+$  is an entire, strictly convex graph.
3. For  $\lambda > \sqrt{5}/2$ ,  $\Sigma_-$  is properly immersed (with infinitely many self-intersections), simply connected and has unbounded distance to the rotation axis.
4. For  $\lambda \leq \sqrt{5}/2$ ,  $\Sigma_-$  is an entire graph. Moreover, if  $\lambda = 1$ ,  $\Sigma_-$  is a horizontal plane (hence minimal and flat), and if  $\lambda \neq 1$ ,  $\Sigma_-$  has positive Gauss-Kronecker curvature.

For rotational  $\mathfrak{h}_\lambda$ -surfaces in  $\mathbb{H}^2 \times \mathbb{R}$  non-intersecting the axis of rotation, we prove the following:

**Theorem 1.3** *Let  $\Sigma$  be a complete, rotational  $\mathfrak{h}_\lambda$ -surface in  $\mathbb{H}^2 \times \mathbb{R}$  non-intersecting the rotation axis. Then,  $\Sigma$  is properly immersed and diffeomorphic to  $\mathbb{S}^1 \times \mathbb{R}$ . Moreover,*

1. If  $\lambda > 1/2$ , then:
  - 1.1. either  $\Sigma$  is the CMC cylinder  $C_\lambda$  of radius  $\arg \tanh\left(\frac{1}{2\lambda}\right)$ , or
  - 1.2. one end converges to  $C_\lambda$  with the same asymptotic behavior as in item 1 in Theorem 1.2, and:
    - a) If  $\lambda > \sqrt{5}/2$ , the other end of  $\Sigma$  has unbounded distance to the rotation axis and self-intersects infinitely many times.
    - b) If  $\lambda \leq \sqrt{5}/2$ , the other end is a graph outside a compact set.
2. If  $\lambda \leq 1/2$ , then both ends are graphs outside compact sets.

## 2 A phase plane analysis of rotational $\mathfrak{h}$ -surfaces in $\mathbb{H}^2 \times \mathbb{R}$

In the development of this section, we regard  $\mathbb{H}^2 \times \mathbb{R}$  as a submanifold of  $\mathbb{R}^3 \times \mathbb{R}$  endowed with the metric  $+, +, -, +$ . Consider a regular curve parametrized by arc-length  $\alpha(s) = (x_1(s), 0, x_3(s), z(s)) \subset \mathbb{H}^2 \times \mathbb{R}$ ,  $x_1(s) > 0$ ,  $s \in I \subset \mathbb{R}$ , contained in a vertical plane passing through the point  $(0, 0, 1, 0)$ , and rotate it around the vertical axis  $\{(0, 0, 1)\} \times \mathbb{R}$ . Since  $x_1^2(s) - x_3^2(s) = -1$ , there exists a  $C^1$  function  $x(s) > 0$  such that

$$\alpha(s) = (\sinh(x(s)), 0, \cosh(x(s)), z(s)).$$

For saving notation, we will simply denote  $\alpha(s)$  by  $(x(s), z(s))$ . Now, note that the image of  $\alpha(s)$  under this 1-parameter group of rotations generates an immersed, rotational surface  $\Sigma$  in  $\mathbb{H}^2 \times \mathbb{R}$  parametrized by

$$\psi(s, \theta) = (\sinh(x(s)) \cos \theta, \sinh(x(s)) \sin \theta, \cosh(x(s)), z(s)) : I \times (0, 2\pi) \rightarrow \mathbb{H}^2 \times \mathbb{R}, \quad (2.1)$$

whose angle function at each point  $\psi(s, \theta)$  is given by  $\nu(\psi(s, \theta)) = x'(s)$ ,  $\forall s \in I$ . Moreover, the principal curvatures on  $\Sigma$  are

$$\kappa_1 = \kappa_\alpha = x'z'' - x''z', \quad \kappa_2 = \frac{z'}{\tanh x}, \quad (2.2)$$

where  $\kappa_\alpha$  stands for the geodesic curvature of the profile curve  $\alpha(s)$ . Thus, the mean curvature of  $\Sigma$  is easily related to the coordinates of  $\alpha(s)$  and bearing in mind that  $x'^2 + z'^2 = 1$ , we get that the function  $x$  is a solution of the autonomous second order ODE

$$x'' = \frac{1 - x'^2}{\tanh x} - 2\varepsilon H_\Sigma \sqrt{1 - x'^2}, \quad \varepsilon = \text{sign}(z'), \quad (2.3)$$

on every subinterval  $J \subset I$  where  $z'(s) \neq 0$  for all  $s \in J$ .

Now, assume that  $\Sigma$  is an  $\mathfrak{h}$ -surface for some  $\mathfrak{h} \in C^1([-1, 1])$ , that is, by using (1.3) we get  $H_\Sigma(\psi(s, \theta)) = \mathfrak{h}(x'(s))$ . Hence, after the change  $y = x'$ , we can rewrite (2.3) as the following autonomous ODE system

$$\begin{pmatrix} x \\ y \end{pmatrix}' = \begin{pmatrix} y \\ \frac{1 - y^2}{\tanh x} - 2\varepsilon \mathfrak{h}(y) \sqrt{1 - y^2} \end{pmatrix} =: F_\varepsilon(x, y). \quad (2.4)$$

At this point, we study this system by using a phase plane analysis as the first author did in [BGM2]. Specifically, the *phase plane* of (2.4) is defined as the half-strip  $\Theta_\varepsilon := (0, \infty) \times (-1, 1)$ , with coordinates  $(x, y)$  denoting, respectively, the distance to the rotation axis and the angle function of  $\Sigma$ . The solutions  $\gamma(s) = (x(s), y(s))$  of system (2.4) are called *orbits*, and the *equilibrium points* are the points  $e_0^\varepsilon = (x_0^\varepsilon, y_0^\varepsilon) \in \Theta_\varepsilon$  such that  $F_\varepsilon(x_0^\varepsilon, y_0^\varepsilon) = 0$ , which must lie in the axis  $y = 0$  according to system (2.4).

Next, we compile some features that can be derived from the study of the phase plane.

**Lemma 2.1** *In the above conditions, the following properties hold:*

1. If  $\varepsilon\mathfrak{h}(0) > 0$ , there is a unique equilibrium  $e_0^\varepsilon = (x_0^\varepsilon, 0)$  of (2.4) in  $\Theta_\varepsilon$  given by

$$x_0^\varepsilon = \arg \tanh \left( \frac{1}{2\varepsilon\mathfrak{h}(0)} \right).$$

This equilibrium generates the right circular cylinder  $\mathbb{S}^1(x_0^\varepsilon) \times \mathbb{R}$  of constant mean curvature  $\mathfrak{h}(0)$  and vertical rulings.

2. The Cauchy problem associated to (2.4) for the initial condition  $(x_0, y_0) \in \Theta_\varepsilon$  has local existence and uniqueness. Thus, the orbits provide a foliation by regular  $C^1$  curves of  $\Theta_\varepsilon$  (or of  $\Theta_\varepsilon - \{e_0^\varepsilon\}$ , in case some  $e_0^\varepsilon$  exists).

3. The instants  $s_0 \in J$  such that  $\kappa_\alpha(s_0) = 0$  are the ones for which  $x''(s_0) = y'(s_0) = 0$ , i.e. those such that  $(x(s_0), y(s_0)) \in \Gamma_\varepsilon := \Theta_\varepsilon \cap \{x = \Gamma_\varepsilon(y)\}$ , where

$$\Gamma_\varepsilon(y) = \arg \tanh \left( \frac{\sqrt{1-y^2}}{2\varepsilon\mathfrak{h}(y)} \right). \quad (2.5)$$

Moreover, the curve  $\Gamma_\varepsilon$  is empty when  $\varepsilon\mathfrak{h}(y) \leq 0$ .

4. The axis  $y = 0$  and the curve  $\Gamma_\varepsilon$  divide  $\Theta_\varepsilon$  into connected components, called monotonicity regions, where the coordinates  $x(s)$  and  $y(s)$  of every orbit are strictly monotonous. Moreover, at each of these regions, we have

$$\text{sign}(\kappa_1) = \text{sign}(-\varepsilon y'(s)), \quad \text{sign}(\kappa_2) = \text{sign}(\varepsilon). \quad (2.6)$$

Let us focus now on the behavior of the orbits of system (2.4) in more detail. Firstly, note that we can view such orbits as vertical graphs  $y = y(x)$  where  $y \neq 0$  (i.e. where  $x' \neq 0$ ), so the chain rule yields

$$y'(s) = \frac{dy}{ds} = \frac{dy}{dx} \frac{dx}{ds} = y'(x)y(x) = \frac{1-y(x)^2}{\tanh x} - 2\varepsilon\mathfrak{h}(y(x))\sqrt{1-y(x)^2}. \quad (2.7)$$

Since at each monotonicity region the sign of the quantity  $y(x)y'(x)$  is constant, the behavior of the orbit passing through some  $(x_0, y_0) \in \Theta_\varepsilon$  is determined by the signs of  $y_0$  and  $\Gamma_\varepsilon(y_0) - x_0$  (whenever  $\Gamma_\varepsilon(y_0)$  exists). We detail it next:

**Lemma 2.2** *In the above conditions, the behavior of the orbit of (2.4) passing through a given point  $(x_0, y_0) \in \Theta_\varepsilon$  such that  $\Gamma_\varepsilon(y_0)$  exists is described as follows:*

1. If  $x_0 > \Gamma_\varepsilon(y_0)$  (resp.  $x_0 < \Gamma_\varepsilon(y_0)$ ) and  $y_0 > 0$ , then  $y(x)$  is strictly decreasing (resp. increasing) at  $x_0$ .
2. If  $x_0 > \Gamma_\varepsilon(y_0)$  (resp.  $x_0 < \Gamma_\varepsilon(y_0)$ ) and  $y_0 < 0$ , then  $y(x)$  is strictly increasing (resp. decreasing) at  $x_0$ .
3. If  $y_0 = 0$ , then the orbit passing through  $(x_0, 0)$  is orthogonal to the  $x$  axis.
4. If  $x_0 = \Gamma_\varepsilon(y_0)$ , then  $y'(x_0) = 0$  and  $y(x)$  has a local extremum at  $x_0$ .

The following result discusses how an orbit  $\gamma(s) = (x(s), y(s)) \in \Theta_\varepsilon$  behaves when  $x(s) \rightarrow \infty$ .

**Proposition 2.3** *Let  $\gamma(s) = (x(s), y(s))$  be an orbit in  $\Theta_\varepsilon$  such that  $(x(s), y(s)) \rightarrow (\infty, y_0)$  when  $|s| \rightarrow \infty$ , with  $y_0 \in (-1, 1)$ . Then,  $2\varepsilon\mathfrak{h}(y_0) = \sqrt{1 - y_0^2}$ .*

*Proof:* Suppose that  $\gamma(s) \in \Theta_\varepsilon$  satisfies  $x(s) \rightarrow \infty$  and  $y(s) \rightarrow y_0 \in (-1, 1)$  when  $|s| \rightarrow \infty$ . Then, there exists  $s_0 \in \mathbb{R}$  such that for every  $s \in \mathbb{R}$  satisfying  $|s| > |s_0|$ ,  $\gamma(s)$  is strictly contained in some monotonicity region and so does not intersect the axis  $y = 0$ . Thus,  $\gamma(s)$  can be written as a vertical graph  $y = y(x)$  satisfying  $y(x) \rightarrow y_0$  and  $y'(x) \rightarrow 0$  as  $x \rightarrow \infty$ , and substituting into Equation (2.7) we get

$$1 - y_0^2 - 2\varepsilon\mathfrak{h}(y_0)\sqrt{1 - y_0^2} = 0$$

concluding the result. □

Additionally, we highlight that the possible endpoints of an orbit are restricted as shown in [BGM2, Theorem 4.1, pp. 13-14].

**Lemma 2.4** *No orbit in  $\Theta_\varepsilon$  can converge to some point of the form  $(0, y)$  with  $|y| < 1$ .*

From this result, we conclude that in case that an orbit converges to the axis  $x = 0$ , it must do it to the points  $(0, \pm 1)$ . However, we point out that the existence of an orbit with endpoint at  $(0, \pm 1)$  can not be guaranteed by solving the Cauchy problem since system (2.4) has a singularity at the points with  $x_0 = 0$ . In this case, we can ensure the existence of such an orbit by using the work of Gálvez and Mira [GaMi2] in which they solved the Dirichlet problem for radial solutions of an arbitrary *fully nonlinear elliptic PDE*. Therefore, it is ensured the existence of rotational  $\mathfrak{h}$ -surfaces in  $\mathbb{H}^2 \times \mathbb{R}$  intersecting the rotation axis in an orthogonal way (see Section 3 in [Bue5] for further details). Furthermore, this fact derives the following result in the phase plane  $\Theta_\varepsilon$ .

**Corollary 2.5** *Let be  $\varepsilon, \delta \in \{-1, 1\}$  such that  $\varepsilon\mathfrak{h}(\delta) > 0$  and denote  $\sigma = \text{sign}(\delta)$ . Then, there exists a unique orbit  $\gamma_\sigma$  in  $\Theta_\varepsilon$  that has  $(0, \delta) \in \overline{\Theta_\varepsilon}$  as an endpoint. There is no such an orbit in  $\Theta_{-\varepsilon}$ .*

The unique rotational  $\mathfrak{h}$ -surface associated to the orbit  $\gamma_\sigma$ , that intersects orthogonally the axis of rotation at some point having unit normal  $\delta\partial_z$ , will be denoted by  $\Sigma_\sigma$ .

### 3 Existence of $\mathfrak{h}$ -bowls and $\mathfrak{h}$ -catenoids in $\mathbb{H}^2 \times \mathbb{R}$

This section is devoted to construct examples of properly embedded rotational  $\mathfrak{h}$ -surfaces in  $\mathbb{H}^2 \times \mathbb{R}$ , under some additional assumptions over the function  $\mathfrak{h} \in C^1([-1, 1])$ . For this purpose, we follow the ideas compiled in Section 3 in [BGM2].

Firstly, we show the existence of entire, strictly convex  $\mathfrak{h}$ -graphs in  $\mathbb{H}^2 \times \mathbb{R}$ . Recall that there exists an entire graph with CMC equal to  $H_0 \in \mathbb{R}$  if and only if  $|H_0| \leq 1/2$ . In addition, there exists a sphere with CMC equal to  $H_0$  if and only if  $|H_0| > 1/2$ .

Regarding  $\mathfrak{h}$ -surfaces, a necessary and sufficient condition to ensure the existence of an  $\mathfrak{h}$ -sphere in  $\mathbb{H}^2 \times \mathbb{R}$  is that  $\mathfrak{h}$  must be an even function satisfying

$$2|\mathfrak{h}(y)| > \sqrt{1-y^2} \quad (3.1)$$

for every  $y \in [-1, 1]$  (see Proposition 3.6 and Theorem 4.1 in [Bue5]). Furthermore, under such hypotheses over  $\mathfrak{h}$ , we must take into account that the existence of an  $\mathfrak{h}$ -sphere in  $\mathbb{H}^2 \times \mathbb{R}$  forbids the existence of entire vertical  $\mathfrak{h}$ -graphs in  $\mathbb{H}^2 \times \mathbb{R}$ , since this fact would yield to a contradiction with the maximum principle. Therefore, we construct the announced  $\mathfrak{h}$ -graphs by assuming the failure of inequality (3.1).

**Proposition 3.1** *Let  $\mathfrak{h}$  be a  $C^1$  function on  $[-1, 1]$ , and suppose that there exists  $y_* \in [0, 1]$  (resp.  $y_* \in [-1, 0]$ ) such that  $2\varepsilon\mathfrak{h}(y_*) = \sqrt{1-y_*^2}$ . Then, there exists an upwards-oriented (resp. downwards-oriented) entire rotational  $\mathfrak{h}$ -graph  $\Sigma$  in  $\mathbb{H}^2 \times \mathbb{R}$ . Moreover:*

1. either  $\Sigma$  is a horizontal plane,
2. or  $\Sigma$  is a strictly convex graph.

*Proof:* If  $y_* = 1$  (resp.  $y_* = -1$ ), then  $\mathfrak{h}(1) = 0$  (resp.  $\mathfrak{h}(-1) = 0$ ), and we choose the surface  $\Sigma$  as the horizontal plane  $\mathbb{H}^2 \times \{t_0\}$ ,  $t_0 \in \mathbb{R}$ , which is minimal. Then, by considering  $\Sigma$  with upwards orientation (resp. downwards orientation), its angle function is  $\nu \equiv 1$  (resp.  $\nu \equiv -1$ ), and so from (1.3) the result is trivial.

Now, suppose that  $2\varepsilon\mathfrak{h}(y_*) = \sqrt{1-y_*^2}$  holds for some  $y_* \in [0, 1]$ , assume  $\mathfrak{h}(1) > 0$  and define  $y_0 := \max\{y \in [0, 1] : 2\mathfrak{h}(y) = \sqrt{1-y^2}\}$ . Note that  $y_0$  is well defined since  $\mathfrak{h}(1) > 0$ , and by continuity  $2\mathfrak{h}(y) > \sqrt{1-y^2}$  if  $y \in (y_0, 1]$ . Hence, the horizontal graph  $\Gamma_1 = \Theta_1 \cap \Gamma_1(y)$  defined by (2.5) has one connected component when we restrict  $\Gamma_1(y)$  to  $(y_0, 1]$ . Moreover, it satisfies  $\Gamma_1(1) = 0$  and  $\Gamma_1(y) \rightarrow \infty$  as  $y \rightarrow y_0$ .

Let us take  $\Lambda := \{(x, y) \in \Theta_1 : y > y_0\}$ , and define  $\Lambda_+ := \{(x, y) \in \Lambda : x > \Gamma_1(y)\}$  and  $\Lambda_- := \{(x, y) \in \Lambda : x < \Gamma_1(y)\}$ . Note that  $\Lambda \setminus \Gamma_1$  is divided into two connected components  $\Lambda_+$  and  $\Lambda_-$ , which are precisely monotonicity regions of  $\Theta_1$  because of item 4 in Lemma 2.1. Indeed, by Lemma 2.2 each orbit  $y = y(x)$  in  $\Lambda_+$  (resp.  $\Lambda_-$ ) satisfies that  $y'(x) < 0$  (resp.  $y'(x) > 0$ ).

Now, from Corollary 2.5 it is known that there exists a unique orbit  $\gamma_+$  in  $\Theta_1$  with  $(0, 1)$  as an endpoint. Additionally, by the aforementioned monotonicity properties and Lemma 2.2 it is clear that  $\gamma_+$  is globally contained in  $\Lambda_+$ . Thus,  $\gamma_+$  can be globally defined by a graph  $y = f(x)$ , where  $f \in C^1([0, \infty))$  satisfies  $f(0) = 1$ ,  $f(x) \rightarrow y_1 \geq y_0$  as  $x \rightarrow \infty$ , and  $f'(x) < 0$  for all  $x > 0$ . As a matter of fact, Proposition 2.3 ensures us that  $y_1 = y_0$  (see Figure 1, left).

Consequently, the  $\mathfrak{h}$ -surface  $\Sigma_+$  generated by the orbit  $\gamma_+$  is an entire rotational graph in  $\mathbb{H}^2 \times \mathbb{R}$ . It remains to prove that  $\Sigma_+$  is strictly convex. On the one hand, since  $\gamma_+$  is totally contained in  $\Theta_1$ , hence  $\varepsilon = 1$ , we deduce by (2.6) that  $\kappa_2$  of  $\Sigma_+$  is everywhere positive. On the other hand,  $\gamma_+$  is totally contained in  $\Lambda_+$ , so (2.6) implies that  $\kappa_1$  of  $\Sigma_+$  is also everywhere positive concluding the proof of this case.

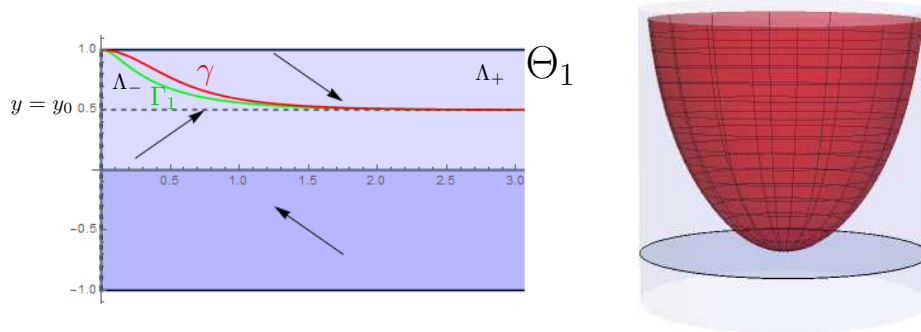


Figure 1: Left: the phase plane  $\Theta_1$ , the regions  $\Lambda_+$  and  $\Lambda_-$ , the curve  $\Gamma_1$  in green and the orbit  $\gamma_+$  in red. Right: an  $\mathfrak{h}$ -bowl in  $\mathbb{H}^2 \times \mathbb{R}$ . The prescribed function is  $\mathfrak{h}(y) = \sqrt{3}(y - 0.25)$ .

To finish, note that the case  $\mathfrak{h}(-1) > 0$ ,  $y_* \leq 0$  is treated analogously; and the two remaining cases,  $\mathfrak{h}(1) < 0$ ,  $y_* \geq 0$  and  $\mathfrak{h}(-1) < 0$ ,  $y_* \leq 0$ , can be reduced to the previous ones by changing the orientation.  $\square$

These  $\mathfrak{h}$ -surfaces will be called  $\mathfrak{h}$ -bowls, in analogy with the theory of self-translating solitons of the mean curvature flow (see [Bue1, Bue2, LiMa]) that we extend with the previous result. See Figure 1, right, for a graphic of an  $\mathfrak{h}$ -bowl in  $\mathbb{H}^2 \times \mathbb{R}$ .

Secondly, we study the existence of *catenoid-type* rotational  $\mathfrak{h}$ -surfaces under appropriate conditions for the prescribed function  $\mathfrak{h}$ .

**Proposition 3.2** *Let  $\mathfrak{h}$  be a  $C^1$  function on  $[-1, 1]$ , and suppose that  $\mathfrak{h} \leq 0$  and  $\mathfrak{h}(\pm 1) = 0$ . Then, there exists a one-parameter family of properly embedded, rotational  $\mathfrak{h}$ -surfaces in  $\mathbb{H}^2 \times \mathbb{R}$  of strictly negative extrinsic curvature at every point, and diffeomorphic to  $\mathbb{S}^1 \times \mathbb{R}$ . Each example is a bi-graph over  $\mathbb{H}^2 - \mathbb{D}_{\mathbb{H}^2}(x_0)$ , where  $\mathbb{D}_{\mathbb{H}^2}(x_0) = \{x \in \mathbb{H}^2 : |x|_{\mathbb{H}^2} < x_0\}$ , for some  $x_0 > 0$ .*

*Proof:* Let  $\Sigma(x_0)$  be the rotational  $\mathfrak{h}$ -surface generated by the arc-length parametrized curve  $\alpha(s) = (x(s), z(s))$  with the following initial conditions

$$x(0) = x_0, \quad z(0) = 0, \quad \text{and} \quad z'(0) = 1, \quad \text{with} \quad x_0 > 0.$$

Then, the orbit  $\gamma(s) = (x(s), y(s))$  of system (2.4) associated to  $\alpha(s)$  passes through the point  $(x_0, 0)$  at  $s = 0$ . Moreover,  $\gamma$  is contained in  $\Theta_1$  around such a point, that is,  $\varepsilon = 1$ .

Observe that the curve  $\Gamma_1$  given by (2.5) does not exist because of the assumption  $\mathfrak{h} \leq 0$ . Consequently, by item 4 in Lemma 2.1 there are two monotonicity regions of  $\Theta_1$  given by  $\Lambda_+ := \{(x, y) \in \Theta_1 : y > 0\}$  and  $\Lambda_- := \{(x, y) \in \Theta_1 : y < 0\}$ . Then, from (2.4) we know that  $\gamma$  satisfies  $x' > 0$  and  $y' > 0$  in  $\Lambda_+$ , and  $x' < 0$  and  $y' > 0$  in  $\Lambda_-$ ; see Figure 2, left.

Let us prove now that  $\gamma$  must be a proper arc strictly contained in  $\Theta_1$  satisfying  $\gamma(s) \rightarrow (\infty, \pm 1)$  as  $s \rightarrow \pm\infty$ . First note that, the assumption  $\mathfrak{h} \leq 0$  implies that given  $y_0 \in (-1, 1)$ , the equation  $2\mathfrak{h}(y_0) = \sqrt{1 - y_0^2}$  has no solutions, so from Proposition 2.3  $\gamma$  cannot satisfy  $\gamma(s) \rightarrow (\infty, y_0)$  as  $s \rightarrow$

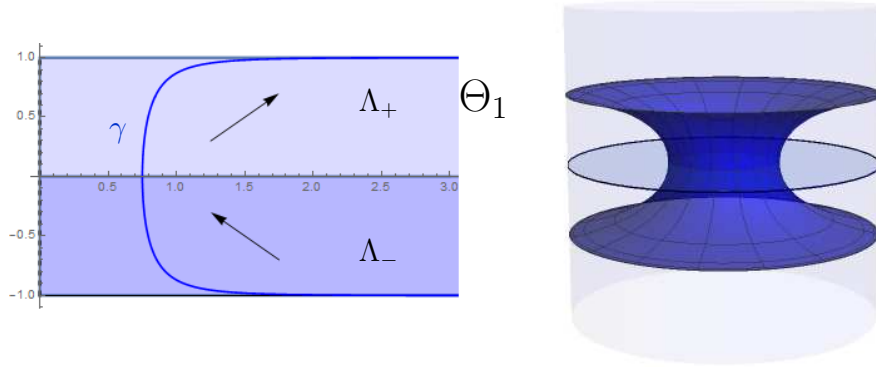


Figure 2: Left: the phase plane  $\Theta_1$ , the monotonicity regions  $\Lambda_+$  and  $\Lambda_-$ , and an orbit  $\gamma$  in blue. Right: an  $\mathfrak{h}$ -catenoid in  $\mathbb{H}^2 \times \mathbb{R}$ . The prescribed function is  $\mathfrak{h}(y) = y^2 - 1$ .

$\pm\infty$ . Second, since  $\mathfrak{h} \in C^1$  and  $\mathfrak{h}(\pm 1) = 0$ , from the uniqueness of the Cauchy problem associated to (2.4), the curve  $(s, \pm 1)$ ,  $s > 0$ , is a solution to (2.4) which corresponds to a horizontal plane  $\mathbb{H}^2 \times \{t_0\}$ ,  $t_0 \in \mathbb{R}$ , endowed with  $\pm \partial_z$  as unit normal, that is,  $\gamma(s)$  cannot satisfy  $\gamma(s_0) = (x_0, \pm 1)$  for some  $s_0 \in \mathbb{R}$ . Finally, it remains to show that  $\gamma(s)$  cannot converge to some  $(x_0, \pm 1)$ ,  $x_0 > 0$ , as  $s \rightarrow \pm\infty$ . Otherwise, there would exist  $s_0 \in \mathbb{R}$  such that for  $|s| > |s_0|$ ,  $x(s)$  is a monotonous function satisfying  $x(s) \rightarrow x_0$  as  $|s| \rightarrow \infty$ . Thus, the mean value theorem ensures us that  $x'(s) = y(s) \rightarrow 0$ , which is a contradiction with the fact that  $y(s) \rightarrow \pm 1$ .

Thus,  $\Sigma(x_0)$  is a bi-graph in  $\mathbb{H}^2 \times \mathbb{R}$  over  $\Omega(x_0) := \mathbb{H}^2 - \mathbb{D}_{\mathbb{H}^2}(x_0)$ , with the topology of  $\mathbb{S}^1 \times \mathbb{R}$ . Indeed,  $\Sigma(x_0) = \Sigma_1 \cup \Sigma_2$  where both  $\Sigma_i$  are graphs over  $\Omega(x_0)$  with  $\partial \Sigma_i = \partial \Omega(x_0)$  and  $\Sigma_i$  meets the horizontal plane  $\mathbb{H}^2 \times \{0\}$  in an orthogonal way along  $\partial \Sigma_i$  (see Figure 2 right).

It remains to prove that the extrinsic curvature of  $\Sigma(x_0)$  is strictly negative. By (2.4) we get  $y'(s) > 0$  for all  $s$ , so from (2.6) we derive  $\kappa_1 < 0$  and  $\kappa_2 > 0$  at every  $p \in \Sigma$ .  $\square$

This one-parameter family of rotational  $\mathfrak{h}$ -surfaces is a generalization of the usual minimal catenoids in  $\mathbb{H}^2 \times \mathbb{R}$ , and this is the reason for calling them  $\mathfrak{h}$ -catenoids. As happens for the minimal catenoids, the  $\mathfrak{h}$ -catenoids are parametrized by their *necksizes*, i.e. the distance of their *waists* to the axis of rotation.

#### 4 Classification of rotational $\mathfrak{h}$ -surfaces with linear prescribed mean curvature

Our aim in this section is to classify the rotational examples of the following class of  $\mathfrak{h}$ -surfaces:

**Definition 4.1** *An oriented surface  $\Sigma$  immersed in  $\mathbb{H}^2 \times \mathbb{R}$  is an  $\mathfrak{h}_\lambda$ -surface if its mean curvature function  $H_\Sigma$  satisfies*

$$H_\Sigma(p) = \mathfrak{h}_\lambda(\nu(p)) = a\nu(p) + \lambda, \quad \forall p \in \Sigma, \quad a, \lambda \in \mathbb{R}. \quad (4.1)$$

Note that if  $a = 0$ , then we are studying surfaces with constant mean curvature equal to  $\lambda$ . Also, if  $\lambda = 0$  the  $\mathfrak{h}_\lambda$ -surfaces are translating solitons of the mean curvature flow, see [Bue1, Bue2, LiMa].

Hence, we suppose that  $a, \lambda$  are not null in order to avoid these cases. After a homothety in  $\mathbb{H}^2 \times \mathbb{R}$  we can suppose  $a = 1$  in Equation (4.1). Moreover, if  $\Sigma$  is an  $\mathfrak{h}_\lambda$ -surface, then  $\Sigma$  with its opposite orientation is an  $\mathfrak{h}_{-\lambda}$ -surface. Therefore, we will assume  $\lambda > 0$  without losing generality. In particular this implies that  $\varepsilon \mathfrak{h}(0) > 0$  if and only if  $\varepsilon = 1$ , and consequently the equilibrium  $e_0 = (\arg \tanh(\frac{1}{2\varepsilon \mathfrak{h}(0)}), 0)$  can only exist in  $\Theta_1$ . The CMC vertical cylinder generated by  $e_0$  will be denoted by  $C_\lambda$ .

First, we announce two technical results that will be useful in the sequel. The first one was originally proved by López in [Lop] for surfaces in  $\mathbb{R}^3$  whose mean curvature is given by Equation (4.1).

**Lemma 4.2** *There do not exist closed  $\mathfrak{h}_\lambda$ -surfaces in  $\mathbb{H}^2 \times \mathbb{R}$ .*

*Proof:* Arguing by contradiction, suppose that  $\Sigma$  is a closed  $\mathfrak{h}_\lambda$ -surface in  $\mathbb{H}^2 \times \mathbb{R}$ . If  $h : \Sigma \rightarrow \mathbb{R}$  denotes the *height function* of  $\Sigma$ , it is known that the Laplace-Beltrami operator  $\Delta_\Sigma$  of  $h$  is  $\Delta_\Sigma h = 2H_\Sigma \langle \eta, \partial_z \rangle$ . Since  $\Sigma$  is an  $\mathfrak{h}_\lambda$ -surface, we get

$$\Delta_\Sigma h = 2 \langle \eta, \partial_z \rangle^2 + 2\lambda \langle \eta, \partial_z \rangle.$$

We integrate this equation in  $\Sigma$ . By the divergence theorem and since  $\partial \Sigma = \emptyset$ , we have

$$0 = \int_\Sigma \langle \eta, \partial_z \rangle^2 d\Sigma + \lambda \int_\Sigma \langle \eta, \partial_z \rangle d\Sigma.$$

The second integral is zero by the divergence theorem, since the constant vector field  $\partial_z$  has zero divergence. So, the first integral vanishes, that is,  $\Sigma$  is contained in a cylindrical surface of the form  $\beta \times \mathbb{R}$ ,  $\beta \subset \mathbb{H}^2$  being a curve, which contradicts that  $\Sigma$  is compact.  $\square$

The second result forbids the existence of closed orbits in the phase plane of system (2.4) for some prescribed functions  $\mathfrak{h}$ . It follows from Bendixson-Dulac theorem, a classical result which appears in most textbooks on differential equations; see e.g. [ADL].

**Theorem 4.3** *Let  $\mathfrak{h}$  be a  $C^1$  function on  $[-1, 1]$  such that  $\mathfrak{h}'(y) \neq 0$ ,  $\forall y \in (-1, 1)$ . Then, there do not exist closed orbits in  $\Theta_\varepsilon$ .*

*Proof:* Let us write system (2.4) as

$$\begin{pmatrix} x \\ y \end{pmatrix}' = \begin{pmatrix} y \\ \frac{1-y^2}{\tanh x} - 2\varepsilon \mathfrak{h}(y) \sqrt{1-y^2} \end{pmatrix} = \begin{pmatrix} P(x, y) \\ Q(x, y) \end{pmatrix},$$

and define the function  $\alpha : \Theta_\varepsilon \rightarrow \mathbb{R}$  and the vector field  $V : \Theta_\varepsilon \rightarrow \Theta_\varepsilon$  as

$$\alpha(x, y) = \frac{\sinh x}{\sqrt{1-y^2}}, \quad V(x, y) = \alpha(x, y)(P(x, y), Q(x, y)).$$

Arguing by contradiction, suppose that there exists some closed orbit  $\bar{\gamma}$  in  $\Theta_\varepsilon$  and name  $\Omega$  to its inner region. A simple computation yields  $\operatorname{div}V = (\alpha P)_x + (\alpha Q)_y = -2\varepsilon\mathfrak{h}'(y)\sinh x$ , which has constant sign since  $x > 0$  in  $\Theta_\varepsilon$  and  $\mathfrak{h}'(y) \neq 0$ . Therefore, the divergence theorem in  $\Omega$  yields

$$0 \neq \int_{\Omega} \operatorname{div}V = \int_{\gamma} \langle V, \mathbf{n}_{\gamma} \rangle = 0,$$

where  $\mathbf{n}_{\gamma}$  is the unit normal to the curve  $\gamma$ . Recall that the last integral vanishes since  $V$  is everywhere tangent to  $\gamma$ . This contradiction proves the result.  $\square$

In particular, the prescribed function  $\mathfrak{h}_{\lambda}(y) = y + \lambda$ ,  $\lambda > 0$  lies in the hypothesis of Theorem 4.3, hence the phase plane  $\Theta_\varepsilon$  of system (2.4) for  $\mathfrak{h}_{\lambda}$ -surfaces does not have closed orbits.

Now, suppose that  $\Sigma$  is a rotational  $\mathfrak{h}_{\lambda}$ -surface generated by an arc-length parametrized curve  $\alpha(s) = (x(s), z(s))$ . Then, (1.3) and (2.2) yields

$$2H_{\Sigma} = 2(x' + \lambda) = x'z'' - x''z' + \frac{z'}{\tanh x}. \quad (4.2)$$

Our first goal is to study the structure of the orbits around  $e_0 = (\arg \tanh(\frac{1}{2\lambda}), 0)$ . Recall that  $e_0$  exists if and only if  $\lambda > 1/2$ ; otherwise,  $\arg \tanh$  is not well defined. The *linearized* system of (2.4) at  $e_0$  is given by

$$\begin{pmatrix} 0 & 1 \\ 1 - 4\lambda^2 & -2 \end{pmatrix}, \quad (4.3)$$

whose eigenvalues are

$$\mu_1 = -1 + \sqrt{2 - 4\lambda^2}, \quad \text{and} \quad \mu_2 = -1 - \sqrt{2 - 4\lambda^2}.$$

From standard theory of non-linear autonomous systems we derive:

**Lemma 4.4** *In the above conditions, we have:*

- If  $\lambda > \frac{\sqrt{2}}{2}$ , then  $\mu_1$  and  $\mu_2$  are complex conjugate with negative real part. Thus,  $e_0$  has an inward spiral structure, and every orbit close enough to  $e_0$  converges asymptotically to it spiraling around infinitely many times.
- If  $\lambda = \frac{\sqrt{2}}{2}$ , then  $\mu_1 = \mu_2 = -1$ . Thus,  $e_0$  is an asymptotically stable improper node, and every orbit close enough to  $e_0$  converges asymptotically to it, maybe spiraling around a finite number of times.
- If  $0 < \lambda < \frac{\sqrt{2}}{2}$ , then  $\mu_1$  and  $\mu_2$  are different and real. Thus,  $e_0$  is an asymptotically stable node and has a sink structure, hence every orbit close enough to  $e_0$  converges asymptotically to it directly, i.e. without spiraling around.

Now we stand in position to prove Theorem 1.2.

*Proof of Theorem 1.2:* Note that the behavior of the orbits in each phase plane  $\Theta_\varepsilon$  depends on the curve  $\Gamma_\varepsilon$  and the monotonicity regions generated by it. Consequently, we analyze three different cases for  $\lambda$ :  $\lambda > \sqrt{5}/2$ ,  $\lambda = \sqrt{5}/2$  and  $0 < \lambda < \sqrt{5}/2$ .

Case  $\lambda > \sqrt{5}/2$

Let us assume  $\lambda > \sqrt{5}/2$ . For  $\varepsilon = 1$ , the curve  $\Gamma_1$  given by (2.5) is a compact connected arc in  $\Theta_1$  joining  $(0, 1)$  and  $(0, -1)$ , whereas for  $\varepsilon = -1$ , since  $\mathfrak{h}$  is positive, the curve  $\Gamma_{-1}$  does not exist in  $\Theta_{-1}$ . As a matter of fact, by item 4 in Lemma 2.1 we know that there are four monotonicity regions in  $\Theta_1$  which will be denoted by  $\Lambda_1, \dots, \Lambda_4$ , and there are only two monotonicity regions in  $\Theta_{-1}$  which will be denoted by  $\Lambda_+$  and  $\Lambda_-$ . See Figure 3.

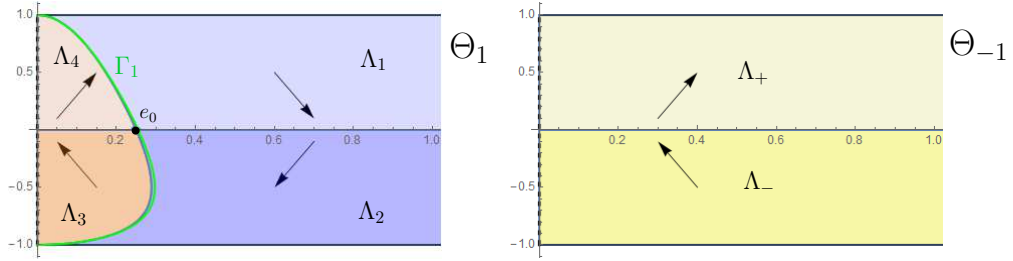


Figure 3: The phase planes  $\Theta_1$  and  $\Theta_{-1}$  for  $\lambda > \sqrt{5}/2$  with their monotonicity regions and the direction of the motion of the orbits at each of them.

Now, by using Corollary 2.5 it is clear that there exists a unique orbit  $\gamma_+$  (resp.  $\gamma_-$ ) in  $\Theta_1$  with  $(0, 1)$  (resp.  $(0, -1)$ ) as an endpoint.

On the one hand, let us study the behavior of  $\gamma_+$ . Firstly, we can suppose that such an orbit satisfies  $\gamma_+(0) = (0, 1)$  in  $\Theta_1$ , i.e., it generates an arc-length parametrized curve  $\alpha_+(s)$  intersecting orthogonally the rotation axis with upwards oriented unit normal at  $s = 0$ . Because of the monotonicity properties,  $\gamma_+(s)$  is strictly contained in the region  $\Lambda_1$  for  $s > 0$  small enough. However, the orbit  $\gamma_+$  cannot stay forever in  $\Lambda_1$ , otherwise  $\gamma_+$  would be globally defined by a graph  $y = f(x)$  such that

$$f(0) = 1, \quad f'(x) < 0 \quad \forall x > 0 \quad \text{and} \quad \lim_{x \rightarrow \infty} f(x) = c \in [0, 1).$$

This contradicts Proposition 2.3 since  $\lambda > \sqrt{5}/2$  and hence  $2\mathfrak{h}_\lambda(y) = 2(y + \lambda) > \sqrt{1 - y^2}$ . Thus,  $\gamma_+(s)$  intersects the axis  $y = 0$  in an orthogonal way at a point  $(x_+, 0)$  with  $x_+ > \arg \tanh\left(\frac{1}{2\lambda}\right)$  at some finite instant  $s_+ > 0$ .

On the other hand, for the orbit  $\gamma_-$  we assume that  $\gamma_-(0) = (0, -1)$  in  $\Theta_1$ , that is, it generates an arc-length parametrized curve  $\alpha_-(s)$  intersecting orthogonally the axis of rotation with downwards oriented unit normal at  $s = 0$ . By an analogous reasoning, we can assert that  $\gamma_-(s)$  intersects  $y = 0$  orthogonally at  $(x_-, 0)$  with  $x_- > \arg \tanh\left(\frac{1}{2\lambda}\right)$  at some finite instant  $s_- < 0$ .

Now, we prove that  $x_+ < x_-$  arguing by contradiction. First, see that if  $x_+ = x_- = \bar{x}$ , by uniqueness of the Cauchy problem the orbits  $\gamma_+$  and  $\gamma_-$  could be smoothly glued together constructing a larger orbit  $\bar{\gamma}$  which would be a compact arc joining the points  $(0, 1)$ ,  $(\bar{x}, 0)$  and  $(0, -1)$  and so the rotational  $\mathfrak{h}_\lambda$ -surface generated would be a rotational  $\mathfrak{h}$ -sphere, which is impossible because of Lemma 4.2. Additionally, if  $x_+ > x_-$ , it would mean that  $\gamma_-$  intersect the axis  $y = 0$  at

the left-hand side of  $\gamma_+$ , and consequently the only possibility for  $\gamma_-$  would be to enter the region  $\Lambda_1$ , later  $\Lambda_4$  and after that  $\Lambda_3$ . In any case,  $\gamma_-$  cannot converge to any point  $(0, y)$ ,  $|y| < 1$  in virtue of Lemma 2.4. Repeating this process, and since  $\gamma_-$  cannot self-intersect nor converge to a closed orbit by Theorem 4.3,  $\gamma_-$  finishes converging asymptotically to the equilibrium  $e_0$  as  $s \rightarrow -\infty$ , spiriling around infinitely many times. This is a contradiction with the inward spiral structure of  $e_0$ , since this orbit would tend to escape from  $e_0$  when  $s$  increases. See Figure 4.

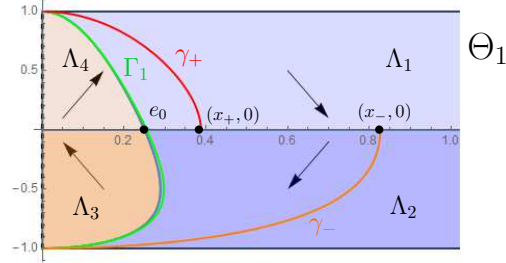


Figure 4: The phase plane  $\Theta_1$  for  $\lambda > \sqrt{5/2}$  with the configuration of the orbits  $\gamma_+$  and  $\gamma_-$ , plotted in red and orange, respectively, until they intersect the axis  $y = 0$ .

Let us continue by analyzing the global behavior of both orbits. Firstly, when  $\gamma_+$  passes through  $(x_+, 0)$ , it enters to  $\Lambda_2$  but cannot intersect  $\gamma_-$ , so  $\gamma_+$  has to enter to  $\Lambda_3$ . After that, due to the monotonicity properties and Lemma 2.4 we deduce that  $\gamma_+$  has to enter to  $\Lambda_4$  and intersect  $\Gamma_1$ . Since  $\gamma_+$  cannot self-intersect nor converge to a limit closed orbit in  $\Theta_1$  in virtue of Theorem 4.3, the only possibility for  $\gamma_+$  is to repeat this behavior and eventually converge asymptotically to the equilibrium  $e_0$  (see the plot of  $\gamma_+$  in Figure 5 top-left). Furthermore, since  $\lambda > \sqrt{2}/2$ ,  $\gamma_+$  spirals around  $e_0$  infinitely many times.

In this way,  $\gamma_+$  generates the curve  $\alpha_+(s) = (x_+(s), z_+(s))$  satisfying: the  $x_+(s)$ -coordinate is bounded by the value  $x_+$  and converges to  $\arg \tanh\left(\frac{1}{2\lambda}\right)$ ; and the  $z_+(s)$ -coordinate is strictly increasing since  $\gamma_+ \subset \Theta_1$ , hence  $z'_+(s) > 0$ . Then,  $\alpha_+(s)$  is an embedded curve that converges to the line  $x = \arg \tanh\left(\frac{1}{2\lambda}\right)$  intersecting it infinitely many times. Therefore, after rotating such a curve around the rotation axis, we derive that the generated surface  $\Sigma_+$  is a properly embedded, simply connected  $\mathfrak{h}_\lambda$ -surface that converges to the CMC cylinder  $C_\lambda$  intersecting it infinitely many times. See  $\Sigma_+$  in Figure 5 top-right.

Now we focus on  $\gamma_-$ , which intersects the axis  $y = 0$  at the point  $\gamma_-(s_-) = (x_-, 0)$  at some finite instant  $s_- < 0$ . So, when the parameter  $s < s_-$  decreases,  $\gamma_-$  enters to  $\Lambda_1$ . Bearing in mind that  $\gamma_+$  and  $\gamma_-$  cannot intersect, from the monotonicity properties we deduce that  $\gamma_-$  has as endpoint  $\gamma_-(s_1) = (x_1, 1)$  with  $0 < x_1 < x_-$  and  $s_1 < s_-$ . Then,  $\gamma_-$  generates the curve  $\alpha_-(s) = (x_-(s), z_-(s))$  satisfying that:  $x_-(s_1) = x_1$  and  $x'_-(s_1) = 1$ , so from (4.2) we get  $z''_-(s_1) > 0$ , i.e., the height of  $\alpha_-$  reaches a minimum at  $s_1$ . If we name  $\Sigma_-$  to the  $\mathfrak{h}_\lambda$ -surface associated to  $\gamma_-$  and generated by rotating  $\alpha_-(s)$ , the image of the points  $\alpha_-(s_1)$  under such rotation corresponds to points on the boundary of  $\Sigma_-$  having unit normal  $\partial_z$ .

Therefore, for  $s < s_1$ ,  $s$  close enough to  $s_1$ , the height function  $z_-(s)$  of  $\alpha_-(s)$  is decreasing, i.e.  $z'_-(s) < 0$ . Consequently,  $\alpha_-(s)$  for  $s < s_1$  close enough to  $s_1$  generates an orbit in  $\Theta_{-1}$  (since  $\varepsilon = \text{sign}(z'_-) = -1$ ), which will be named  $\gamma_-$  for saving notation. Hence, the orbit  $\gamma_-(s)$  continues

from  $\Theta_1$  to  $\Theta_{-1}$  as  $s$  decreases from  $s = s_1$ . At this point, the continuation of  $\gamma_-$  between the phase planes  $\Theta_{\pm 1}$  has to be understood as the extension of  $\Sigma_-$  by solving the Cauchy problem for rotational vertical  $\mathfrak{h}_\lambda$ -graphs having the same vertical unit normal.

Hence,  $\gamma_-(s)$  belongs to  $\Theta_{-1}$  for  $s < s_1$  close enough to  $s_1$  and lies in the region  $\Lambda_+$ . Once again, by monotonicity,  $\gamma_-$  must intersect the axis  $y = 0$  orthogonally and enter to  $\Lambda_-$ . As  $\gamma_-$  cannot stay forever in  $\Lambda_-$  with  $x_-(s) \rightarrow \infty$  for  $s \rightarrow -\infty$ , we derive that there exists  $s_2 < s_1$  such that  $\gamma_-(s_2) = (x_2, -1)$  (see the plot of  $\gamma_-$  in Figure 5 left). Repeating this process indefinitely, we construct a complete, arc-length parametrized curve  $\alpha_-(s)$  with infinitely many self-intersections, whose height function increases and decreases until reaching the rotation axis. Hence, the generated rotational  $\mathfrak{h}_\lambda$ -surface  $\Sigma_-$  is properly immersed (with self-intersections) and simply connected. See Figure 5, bottom right.

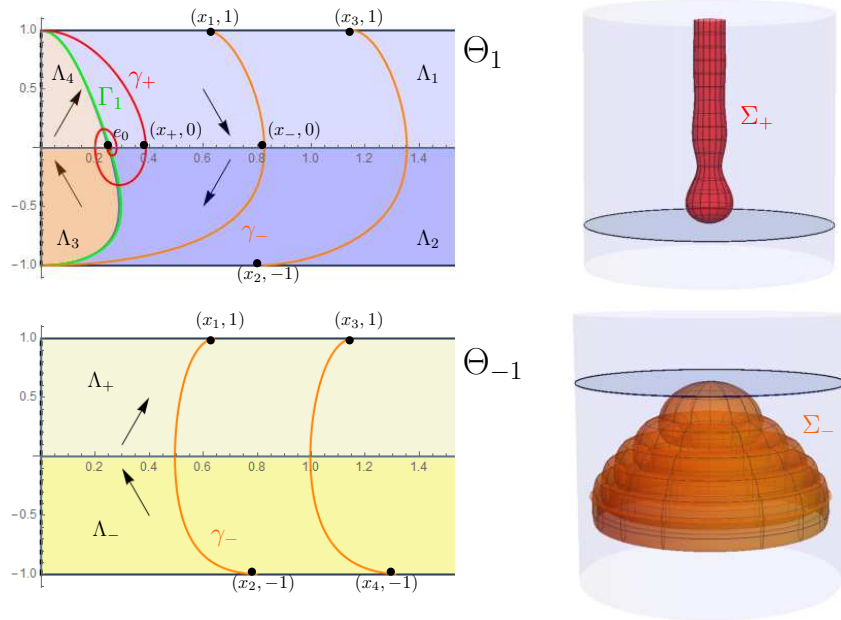


Figure 5: Left: the phase planes  $\Theta_1$  and  $\Theta_{-1}$  for  $\lambda > \sqrt{5}/2$  and the orbits  $\gamma_+$  and  $\gamma_-$ , plotted in red and orange, respectively. Right: the corresponding rotational  $\mathfrak{h}_\lambda$ -surfaces  $\Sigma_+$  and  $\Sigma_-$ .

### Case $\lambda = \sqrt{5}/2$

Assume that  $\lambda = \sqrt{5}/2$ . For  $\varepsilon = 1$ ,  $\Gamma_1$  is formed by two connected arcs  $\Gamma_1^\pm$ , each of them having the point  $(0, \pm 1)$  as endpoint respectively, and both having the line  $y = -2/\sqrt{5}$  as an asymptote. From item 4 in Lemma 2.1 we find five monotonicity regions in the phase plane  $\Theta_1$  denoted by  $\Lambda_1, \dots, \Lambda_5$  (see Figure 6 left). For  $\varepsilon = -1$ , the phase plane  $\Theta_{-1}$  is exactly the same that in the previous case  $\lambda > \sqrt{5}/2$ .

From Corollary 2.5 we can assert that there exists a unique orbit  $\gamma_+$  (resp.  $\gamma_-$ ) in  $\Theta_1$  with  $(0, 1)$  (resp.  $(0, -1)$ ) as an endpoint.

Regarding the orbit  $\gamma_+$ , it converges to  $e_0 = (\operatorname{argtanh} \frac{1}{\sqrt{5}}, 0)$  as  $s \rightarrow \infty$  spiraling around it

infinitely many times in the same fashion as the orbit  $\gamma_+$  studied in the previous case  $\lambda > \sqrt{5}/2$ , see Figure 6 left. Consequently, its corresponding  $\mathfrak{h}_\lambda$ -surface  $\Sigma_+$  has the same behavior as the one shown in Figure 5, top right.

Now, consider the orbit  $\gamma_-$  such that  $\gamma_-(0) = (0, -1)$ . It is clear that  $\gamma_-(s)$  is totally contained in  $\Lambda_3$  and when the parameter  $s$  tends to  $-\infty$ , the orbit  $\gamma_-(s)$  converges to the line  $y = -2/\sqrt{5}$ . Note that  $\gamma_-(s)$  cannot converge to other line  $y = y_0$ ,  $y_0 \in (-1, -2/\sqrt{5})$  in virtue of Proposition 2.3 (see the plot of  $\gamma_-$  in Figure 6 left). Therefore, the generated  $\mathfrak{h}_\lambda$ -surface  $\Sigma_-$  is an entire, strictly convex graph whose angle function tends to the value  $-2/\sqrt{5}$ . See Figure 6 right.

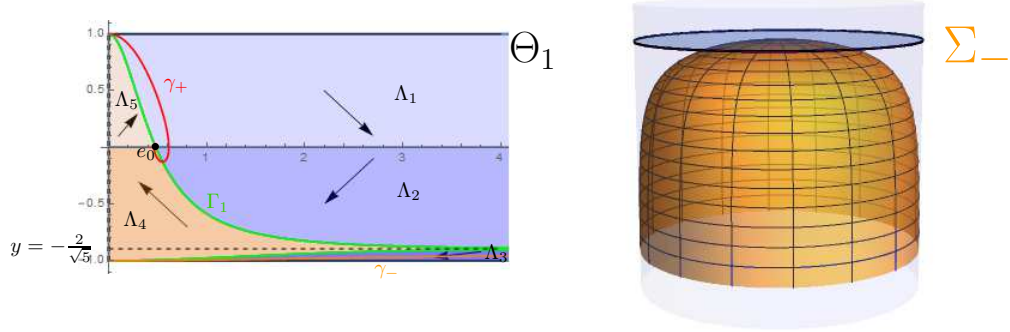


Figure 6: Left: the phase plane  $\Theta_1$  for  $\lambda = \sqrt{5}/2$  and the orbits  $\gamma_+$  and  $\gamma_-$ , plotted in red and orange, respectively. Right: the corresponding rotational  $\mathfrak{h}_\lambda$ -surface  $\Sigma_-$ .

#### Case $\lambda < \sqrt{5}/2$

We begin by analyzing the behavior of  $\Gamma_\varepsilon$  in  $\Theta_\varepsilon$ . Recall that the equilibrium  $e_0$  exists in  $\Theta_1$  if and only if  $\lambda > 1/2$ . Additionally, we define the candidates of asymptotes for  $\Gamma_\varepsilon$  as:

$$y_0^+ := \frac{1}{5}(-4\lambda + \sqrt{5 - 4\lambda^2}), \quad \text{and} \quad y_0^- := \frac{1}{5}(-4\lambda - \sqrt{5 - 4\lambda^2}).$$

Let us distinguish further cases of  $\lambda$ :

1. If  $\lambda > 1$ , then  $\Gamma_1$  is a disconnected arc having two connected components  $\Gamma_1^+$  and  $\Gamma_1^-$ , with  $\Gamma_+$  (resp.  $\Gamma_-$ ) having the point  $(0, 1)$  (resp.  $(0, -1)$ ) as an endpoint and the line  $y = y_0^+$  (resp.  $y = y_0^-$ ) as asymptote; see Figure 7. The curve  $\Gamma_{-1}$  does not exist in  $\Theta_{-1}$  as in the previous cases.

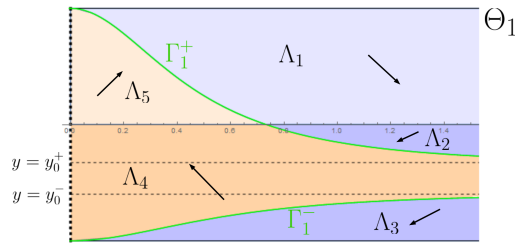


Figure 7: The phase plane  $\Theta_1$  for some  $\lambda \in (1, \sqrt{5}/2)$ .

2. If  $\lambda = 1$ , then  $\Gamma_1$  is a connected arc having  $(0, 1)$  as endpoint and the line  $y = y_0^+ = -3/5$  as asymptote. The line  $y = y_0^- = -1$  does not appear. The curve  $\Gamma_{-1}$  does not exist in  $\Theta_{-1}$ .
3. If  $\lambda < 1$ , then  $\Gamma_1$  is a connected arc having  $(0, 1)$  as endpoint and the line  $y = y_0^+$  as asymptote. Moreover,  $y_0^+ \geq 0$  if and only if  $\lambda \leq 1/2$ . The curve  $\Gamma_{-1}$  is a connected arc having  $(0, -1)$  as endpoint and the line  $y = y_0^-$  as an asymptote; see Figure 8.

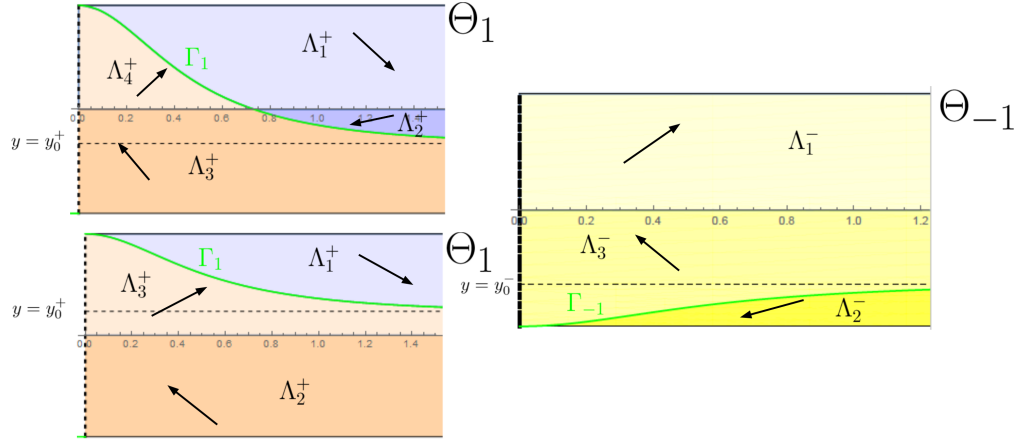


Figure 8: Top left: the phase plane  $\Theta_1$  for  $\lambda > 1/2$ . Bottom left: the phase plane  $\Theta_1$  for  $\lambda \leq 1/2$ . Right: the phase plane  $\Theta_{-1}$  for  $\lambda < 1$ .

Now, we study the behavior of the orbits. Once again, the existence of the orbit  $\gamma_+(s)$  in  $\Theta_1$  such that  $\gamma(0) = (0, 1)$  follows from Corollary 2.5. Then, if we suppose that  $\lambda \leq 1/2$ ,  $\gamma_+(s)$  stays in  $\Lambda_1^+$  as it converges to the line  $y = y_0^+$ , and so  $\Sigma_+$  is an entire, strictly convex graph. Otherwise, i.e., if  $\lambda > 1/2$ , the equilibrium  $e_0$  exists. Since no closed orbit exists in virtue of Theorem 4.3,  $\gamma_+$  converges to  $e_0$  as  $s \rightarrow \infty$ , and its behavior is detailed in Lemma 4.4. Consequently,  $\Sigma_+$  is a properly embedded, simply connected  $\mathfrak{h}_\lambda$ -surface and:

- If  $\lambda > \frac{\sqrt{2}}{2}$ ,  $\Sigma_+$  intersects  $C_\lambda$  infinitely many times.
- If  $\lambda = \frac{\sqrt{2}}{2}$ ,  $\Sigma_+$  intersects  $C_\lambda$  a finite number of times.
- If  $\lambda < \frac{\sqrt{2}}{2}$ ,  $\Sigma_+$  is a strictly convex graph contained in the solid cylinder bounded by  $C_\lambda$  and converging asymptotically to it.

For the study of the orbit  $\gamma_-(s)$  such that  $\gamma_-(0) = (0, -1)$  we have to distinguish between the cases  $\lambda > 1$ ,  $\lambda = 1$ ,  $\lambda < 1$ . This discussion will deeply influence the outcome of Corollary 2.5:

1. If  $\lambda > 1$ , then  $\mathfrak{h}_\lambda(-1) > 0$  and  $\gamma_-(s)$  lies in  $\Theta_1$ .
2. If  $\lambda = 1$ , then  $\mathfrak{h}_\lambda(-1) = 0$  and  $\gamma_-(s)$  does not exist in either  $\Theta_1$  or  $\Theta_{-1}$ .

3. If  $\lambda < 1$ , then  $\mathfrak{h}_\lambda(-1) < 0$  and  $\gamma_-(s)$  lies in  $\Theta_{-1}$ .

If  $\lambda = 1$ , horizontal minimal planes downwards oriented are  $\mathfrak{h}_1$ -surfaces. Consequently, the uniqueness of the Cauchy problem of (2.4) extends to the line  $y = -1$  and so no orbit can have an endpoint at this line.

If  $\lambda \neq 1$ , by monotonicity and Proposition 2.3, the only possibility for  $\gamma_-(s)$  is to converge to the line  $y = y_0^-$ , and so  $\Sigma_-$  is a downwards oriented, strictly convex, entire graph. For  $\lambda > 1$ , the height of  $\Sigma_-$  tends to minus infinity; for  $\lambda < 1$ , the height of  $\Sigma_-$  tends to infinity.

This concludes the classification of the rotational  $\mathfrak{h}_\lambda$ -surfaces that intersect the axis of rotation.  $\square$

To finish, we prove Theorem 1.3.

*Proof of Theorem 1.3:* First, the equilibrium  $e_0 = (\operatorname{arctanh}(\frac{1}{2\lambda}), 0)$  exists if and only if  $\lambda > \frac{1}{2}$ . This equilibrium generates the cylinder  $C_\lambda$  with CMC equal to  $\lambda$  and vertical rulings. For the remaining  $\mathfrak{h}_\lambda$ -surfaces, we distinguish again three cases depending on  $\lambda$ . Take into account that the structure of the phase planes  $\Theta_1$  and  $\Theta_{-1}$  has been just studied in the previous proof. See Figure 3 for  $\lambda > \sqrt{5}/2$ , Figure 6 for  $\lambda = \sqrt{5}/2$  and Figures 7 and 8 for  $\lambda < \sqrt{5}/2$ .

Case  $\lambda > \sqrt{5}/2$

Let us take  $x_0 > \operatorname{arctanh}(\frac{1}{2\lambda})$  and let  $\gamma(s)$  be the orbit in  $\Theta_1$  passing through the point  $(x_0, 0)$  at the instant  $s = 0$ . For  $s < 0$ ,  $\gamma$  has as endpoint some  $(x_1, 1)$ ,  $x_1 > 0$  (if  $x_1 = 0$ ,  $\gamma = \gamma_+$ ), and for  $s > 0$  either converges to  $e_0$  as  $s \rightarrow \infty$  or has another endpoint of the form  $(x_2, -1)$ ,  $x_2 > 0$  (again, if  $x_2 = 0$ ,  $\gamma = \gamma_-$ ). In the second case, the orbit  $\gamma$  continues in  $\Theta_{-1}$  as a compact arc and then goes again in  $\Theta_1$ ; see Figure 9, left. After a finite number of iterations, the orbit  $\gamma$  eventually converges to  $e_0$  spiraling around it infinitely many times.

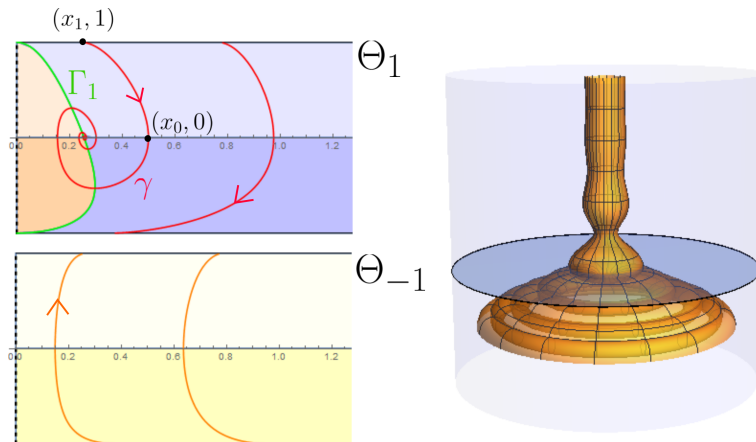


Figure 9: Left: the phase planes  $\Theta_1$  and  $\Theta_{-1}$  for  $\lambda > \sqrt{5}/2$  and an orbit  $\gamma$ . Right: the rotational  $\mathfrak{h}_\lambda$ -surface corresponding to  $\gamma$ .

This configuration ensures us that the  $\mathfrak{h}_\lambda$ -surface generated by  $\gamma$  is properly immersed, non-embedded, and diffeomorphic to  $\mathbb{S}^1 \times \mathbb{R}$ . One end converges to  $C_\lambda$  intersecting it infinitely many times, and the other end has unbounded distance to the axis of rotation, looping and self-intersecting infinitely many times (see Figure 9, right).

Case  $\lambda = \sqrt{5}/2$

Firstly, let us fix some  $x_0 > \arg \tanh(\frac{1}{\sqrt{5}})$  and consider the orbit  $\gamma_1(s)$  passing through  $(x_0, 0)$  at  $s = 0$ . For  $s < 0$ ,  $\gamma_1(s)$  is contained in  $\Lambda_1$ , so it satisfies  $\gamma_1(s_1) = (x_1, 1)$  as endpoint for some  $s_1 < 0$ . Hence, for  $s < s_1$ ,  $\gamma_1(s)$  lies in  $\Theta_{-1}$  and is a compact arc whose other endpoint is located at some  $\gamma_1(s_2) = (x_2, -1)$ . Finally, for  $s < s_2$ ,  $\gamma_1(s)$  lies in the monotonicity region  $\Lambda_3$  in  $\Theta_1$  and stays there as it converges to the line  $y = -2/\sqrt{5}$  as  $s \rightarrow -\infty$ ; see Figure 10, top left, the red orbit.

For  $s > 0$ ,  $\gamma_1(s)$  enters to  $\Lambda_2$ , then goes inside  $\Lambda_4$  and intersects  $y = 0$  for the second time in some  $(\hat{x}_0, 0)$  with  $\hat{x}_0 > 0$ . It is clear that when  $x_0$  increases, then  $\hat{x}_0$  decreases and so  $\hat{x}_0 \rightarrow x_\infty \geq 0$  as  $x_0 \rightarrow \infty$ . Also, note that  $\gamma_1(s)$  stays always above the line  $y = -2/\sqrt{5}$  since the minimum of its  $y(s)$ -coordinate is at the intersection of  $\gamma_1(s)$  with  $\Gamma_1$ . In this setting, we claim that  $x_\infty > 0$ .

Arguing by contradiction, suppose that  $x_\infty = 0$  and consider an orbit  $\sigma(s)$  such that  $\sigma(0)$  lies in  $\Lambda_4$  and is located below the line  $y = -2/\sqrt{5}$ . Then, for  $s > 0$  in virtue of Proposition 2.4 and by monotonicity,  $\sigma(s)$  has to reach the axis  $y = 0$  at a point  $(\hat{r}_1, 0)$  for some finite instant. Due to the definition of  $x_\infty$  and the assumption  $x_\infty = 0$ , there exists  $r > e_0$  and an orbit  $\gamma$  such that  $\gamma(0) = (r, 0)$  and  $\gamma(s_1) = (\hat{r}, 0)$  with  $0 < \hat{r} < \hat{r}_1$ , for some  $s_1 > 0$ . Hence,  $\sigma$  and  $\gamma$  intersect each other, which is a contradiction with the uniqueness of the Cauchy problem.

Secondly, let be  $r_0 > 0$  and take  $\gamma_2(s)$  the orbit such that  $\gamma_2(0) = (r_0, -\sqrt{2}/5)$ . For  $s < 0$ ,  $\gamma_2(s)$  lies in  $\Lambda_4$ , intersects the curve  $\Gamma_1^-$ , enters  $\Lambda_3$  and converges to the line  $y = -2/\sqrt{5}$ . For  $s > 0$ ,  $\gamma_2(s)$  lies in  $\Lambda_4$  until intersecting  $y = 0$  at some  $(\tilde{r}_0, 0)$ . Moreover, as  $r_0$  increases  $\tilde{r}_0$  also increases, and so  $\tilde{r}_0 \rightarrow r_\infty$  as  $r_0 \rightarrow \infty$ . In particular,  $r_\infty \leq x_\infty$ . For  $s \rightarrow \infty$ ,  $\gamma_2(s)$  converges asymptotically to  $e_0$ , spiraling around it infinitely many times; see Figure 10, top left, the blue orbit.

Finally, take some  $\xi_0 \in [r_\infty, x_\infty]$  and let  $\gamma_3(s)$  be the orbit such that  $\gamma_3(0) = (\xi_0, 0)$ . For  $s > 0$  it is clear that  $\gamma_3(s)$  converges asymptotically to  $e_0$ , spiraling around it infinitely many times. Because of how  $r_\infty$  and  $x_\infty$  have been defined, for  $s < 0$  the orbit  $\gamma_3(s)$  cannot intersect  $\Gamma_1^-$  nor intersect  $y = -2/\sqrt{5}$ . Thus, the only possibility for  $\gamma_3(s)$  is to converge to the line  $y = -2/\sqrt{5}$  with strictly decreasing  $y(s)$ -coordinate; see Figure 10, top left, the purple orbit.

Thus, each orbit  $\gamma_i$ ,  $i = 1, 2, 3$  generates a properly immersed  $\mathfrak{h}_\lambda$ -surface  $\Sigma_i$ , diffeomorphic to  $\mathbb{S}^1 \times \mathbb{R}$ , with one end converging asymptotically to the CMC cylinder  $C_\lambda$  and the other being a graph outside a compact set. Moreover,  $\Sigma_1$  is non-embedded, while  $\Sigma_2$  and  $\Sigma_3$  have monotonous height and in particular are embedded; see Figure 10, bottom.

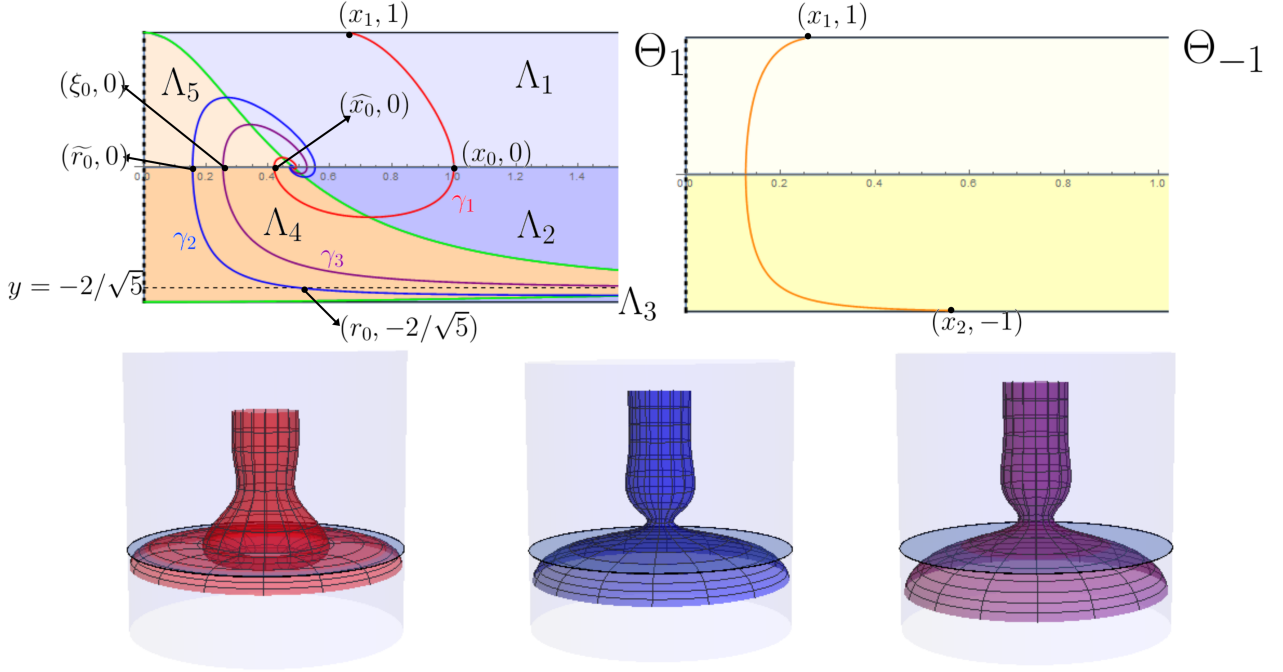


Figure 10: Top: the phase planes  $\Theta_1$  and  $\Theta_{-1}$  for  $\lambda = \sqrt{5}/2$  and the three types of orbits  $\gamma_1$ ,  $\gamma_2$  and  $\gamma_3$ . Bottom: the three corresponding types of rotational  $\mathfrak{h}_\lambda$ -surfaces.

### Case $\lambda < \sqrt{5}/2$

In this final case, we also distinguish between values of  $\lambda$ . Note that the equilibrium  $e_0 = (\arg \tanh(\frac{1}{2\lambda}), 0)$  exists if and only if  $\lambda > 1/2$ . Again, we define

$$y_0^+ := \frac{1}{5}(-4\lambda + \sqrt{5 - 4\lambda^2}), \quad \text{and} \quad y_0^- := \frac{1}{5}(-4\lambda - \sqrt{5 - 4\lambda^2}).$$

1. Case  $1 \leq \lambda < \sqrt{5}/2$ . The structure of the phase plane  $\Theta_1$  (resp.  $\Theta_{-1}$ ) is the same as the one in Figure 7 (resp. Figure 3, right). Recall that  $y_0^- = -1$  in  $\Theta_1$  for  $\lambda = 1$  and there are only four monotonicity regions. The same reasoning as in the case  $\lambda = \sqrt{5}/2$  ensures us that we can construct three types of orbits (see Figure 10) and also the points  $x_\infty$  and  $r_\infty$ :

- $\gamma_1(s)$  such that  $\gamma_1(0) = (x_0, 0)$  with  $x_0 > \arg \tanh(\frac{1}{2\lambda})$  and  $\gamma_1(s) \rightarrow e_0$  as  $s \rightarrow \infty$ .
- $\gamma_2(s)$  such that  $\gamma_2(0) = (r_0, y_0^+)$  with  $r_0 > 0$ ,  $\gamma_2(s) \rightarrow e_0$  as  $s \rightarrow \infty$  and  $\gamma_2(s) \rightarrow y_0^-$  as  $s \rightarrow -\infty$ .
- $\gamma_3(s)$  such that  $\gamma_3(0) = (\xi_0, 0)$  with  $\xi_0 \in [r_\infty, x_\infty]$ ,  $\gamma_3(s) \rightarrow e_0$  as  $s \rightarrow \infty$  and  $\gamma_3(s) \rightarrow y_0^+$  as  $s \rightarrow -\infty$ .

Again, each orbit  $\gamma_i$ ,  $i = 1, 2, 3$  generates a properly immersed  $\mathfrak{h}_\lambda$ -surface  $\Sigma_i$  that is diffeomorphic to  $\mathbb{S}^1 \times \mathbb{R}$ , with one end converging asymptotically to the CMC cylinder  $C_\lambda$  and the other being a graph outside a compact set. Moreover,  $\Sigma_1$  self-intersects, while  $\Sigma_2$  and  $\Sigma_3$  have monotonous height and in particular are embedded.

2. Case  $1/2 < \lambda < 1$ . In this case, the structure of  $\Theta_1$  and  $\Theta_{-1}$  is shown in Figure 8 top left and right respectively. There are also three kind of orbits  $\gamma_1(s), \gamma_2(s), \gamma_3(s)$  in  $\Theta_1$ , and  $\gamma_1(s)$  and  $\gamma_3(s)$  behave as shown in Figure 10. The only difference here is that the orbit  $\gamma_2(s)$  intersects the line  $y = -1$  at a finite point as  $s$  decreases. Then,  $\gamma_2(s)$  enters to  $\Theta_{-1}$  and converges to the line  $y = y_0^-$  as  $s \rightarrow -\infty$ .

The corresponding  $\mathfrak{h}_\lambda$ -surfaces are also similar to the ones constructed in the previous case.

3. Case  $\lambda \leq 1/2$ . In this case, the structure of  $\Theta_1$  and  $\Theta_{-1}$  is shown in Figure 8 bottom left and right respectively. In particular, no equilibrium point exists and the behavior of the orbits is different from the previous cases.

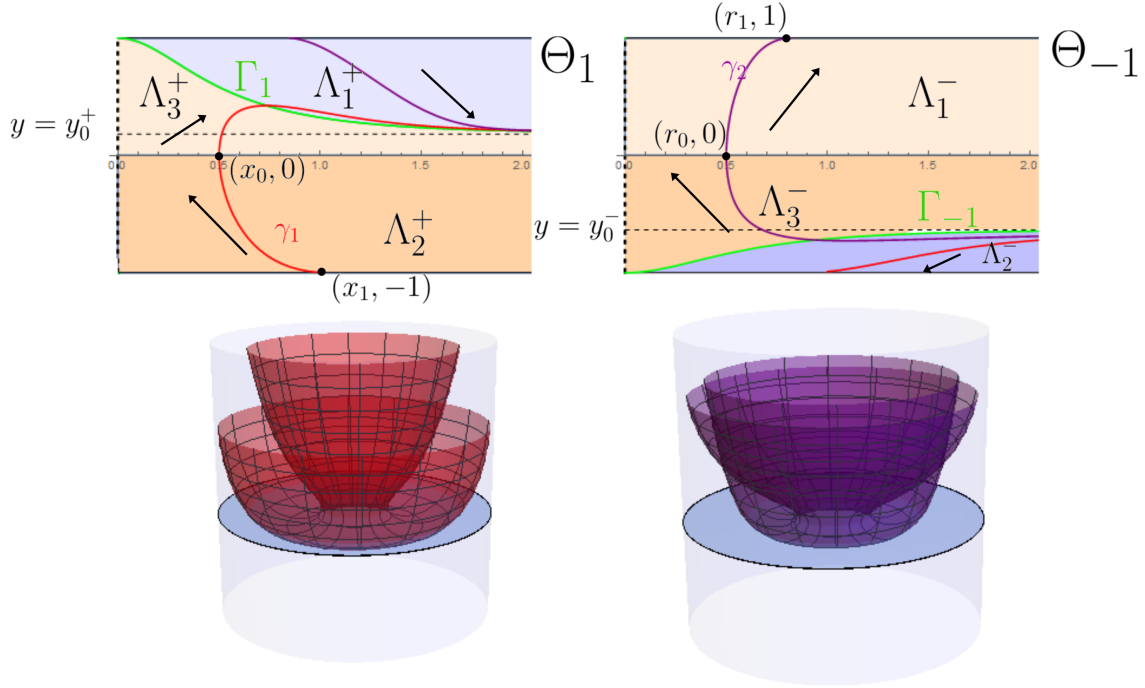


Figure 11: Top: the phase planes  $\Theta_1$  and  $\Theta_{-1}$  for  $\lambda = 1/3$ . Bottom: the two corresponding  $\mathfrak{h}_\lambda$ -surfaces for  $\lambda = 1/3$ .

First, let be  $x_0 > 0$  and  $\gamma_1(s)$  the orbit in  $\Theta_1$  such that  $\gamma_1(0) = (x_0, 0)$ . For  $s > 0$ ,  $\gamma_1(s)$  enters to  $\Lambda_3^+$ , intersects  $\Gamma_1$  and then lies in  $\Lambda_1^+$  converging to the line  $y = y_0^+$ . For  $s < 0$ , the orbit  $\gamma_1(s)$  lies in  $\Lambda_2^+$  and has some  $\gamma_1(s_0) = (x_1, -1)$  as endpoint. Thus,  $\gamma_1(s)$  for  $s < s_0$  lies in  $\Lambda_2^-$  and stays there converging to the line  $y = y_0^-$  as  $s \rightarrow -\infty$ . See Figure 11, the orbit in red.

Lastly, let be  $r_0 > 0$  and  $\gamma_2(s)$  the orbit in  $\Theta_{-1}$  such that  $\gamma_2(0) = (r_0, 0)$ . For  $s < 0$ ,  $\gamma_2(s)$  enters the region  $\Lambda_3^-$  and ends up converging to the line  $y = y_0^-$  as  $s \rightarrow -\infty$ . For  $s > 0$ ,  $\gamma_2(s)$  enters the region  $\Lambda_1^-$  and has as endpoint some  $\gamma_2(s_0) = (r_1, 1)$ . Then,  $\gamma_2(s)$  for  $s > s_0$  lies in  $\Lambda_1^+$  and stays there as it converges to the line  $y = y_0^+$  as  $s \rightarrow \infty$ . See Figure 11, the orbit in purple.

Again, we have two distinct  $\mathfrak{h}_\lambda$ -surfaces  $\Sigma_1$  and  $\Sigma_2$  generated by the orbits  $\gamma_1$  and  $\gamma_2$ . Each  $\Sigma_i$

is properly immersed and diffeomorphic to  $\mathbb{S}^1 \times \mathbb{R}$ , and both ends are graphs outside compact sets. Moreover,  $\Sigma_1$  is embedded, while  $\Sigma_2$  self intersects; see Figure 11, bottom.

□

## References

- [AbRo] U. Abresch, H. Rosenberg, A Hopf differential for constant mean curvature surfaces in  $\mathbb{S}^2 \times \mathbb{R}$  and  $\mathbb{H}^2 \times \mathbb{R}$ , *Acta Math.* **193** (2004), 141–174.
- [Ale] A.D. Alexandrov, Uniqueness theorems for surfaces in the large, I, *Vestnik Leningrad Univ.* **11** (1956), 5–17. (English translation): Amer. Math. Soc. Transl. **21** (1962), 341–354.
- [ADL] J. C. Artés, F. Dumortier, J. Llibre. Qualitative theory of planar differential systems. *Universitext. Springer-Verlag*, Berlin, 2006.
- [BCMR] V. Bayle, A. Cañete, F. Morgan, C. Rosales, On the isoperimetric problem in Euclidean space with density, *Calc. Var. Partial Diff. Equations* **31** (2008), 27–46.
- [Bue1] A. Bueno, Translating solitons of the mean curvature flow in the space  $\mathbb{H}^2 \times \mathbb{R}$ , *J. Geom.* **109** (2018).
- [Bue2] A. Bueno, Uniqueness of the translating bowl in  $\mathbb{H}^2 \times \mathbb{R}$ , *J. Geom.*, **111** (2020).
- [Bue3] A. Bueno, The Björling problem for prescribed mean curvature surfaces in  $\mathbb{R}^3$ , *Ann. Global Anal. Geom.*, **56** (2019), 87-96.
- [Bue4] A. Bueno, Half-space theorems for properly immersed surfaces in  $\mathbb{R}^3$  with prescribed mean curvature, *Ann. Mat. Pura. Appl.*, **199** (2020), 425–444.
- [Bue5] A. Bueno, A Delaunay-type classification result for prescribed mean curvature surfaces in  $\mathbb{M}^2(\kappa) \times \mathbb{R}$ , preprint, [arXiv:1807.10040](https://arxiv.org/abs/1807.10040).
- [Bue6] A. Bueno, Properly embedded surfaces with prescribed mean curvature in  $\mathbb{H}^2 \times \mathbb{R}$ , *Ann. Global Anal. Geom.*, (2020), to appear. DOI:<https://doi.org/10.1007/s10455-020-09741-6>.
- [BGM1] A. Bueno, J.A. Gálvez, P. Mira, The global geometry of surfaces with prescribed mean curvature in  $\mathbb{R}^3$ , *Trans. Amer. Math. Soc.* **373** (2020), 4437-4467.
- [BGM2] A. Bueno, J.A. Gálvez, P. Mira, Rotational hypersurfaces of prescribed mean curvature, *J. Differential Equations* **268** (2020), 2394–2413.
- [BuOr] A. Bueno, I. Ortiz, Invariant hypersurfaces with linear prescribed mean curvature, *J. Math. Anal. Appl.*, **487** (2020).
- [Chr] E.B. Christoffel, Über die Bestimmung der Gestalt einer krummen Oberfläche durch lokale Messungen auf derselben. *J. Reine Angew. Math.* **64** (1865), 193–209.
- [GaMil] J.A. Gálvez, P. Mira, Uniqueness of immersed spheres in three-manifolds, *J. Differential Geometry*, to appear. [arXiv:1603.07153](https://arxiv.org/abs/1603.07153).

- [GaMi2] J.A. Gálvez, P. Mira, Rotational symmetry of Weingarten spheres in homogeneous three-manifolds *J. Reine Angew. Math.*, to appear. [arXiv:1807.09654](https://arxiv.org/abs/1807.09654).
- [GuGu] B. Guan, P. Guan, Convex hypersurfaces of prescribed curvatures, *Ann. Math.* **156** (2002), 655–673.
- [HLR] D. Hoffman, J. De Lira, H. Rosenberg, Constant mean curvature surfaces in  $\mathbb{M}^2 \times \mathbb{R}$ , *Trans. Amer. Math. Soc.* **358** (2006), no. 2, 491–507.
- [HsHs] W. T. Hsiang, W. Y. Hsiang, On the uniqueness of isoperimetric solutions and imbedded soap bubbles in non-compact symmetric spaces, *Invent. Math.* **85** (1989), 39–58.
- [Ilm] T. Ilmanen, Elliptic regularization and partial regularity for motion by mean curvature, *Mem. Amer. Math. Soc.* **108** (1994).
- [LeRo] C. Leandro, H. Rosenberg. Removable singularities for sections of Riemannian submersions of prescribed mean curvature, *Bull. Sci. Math.* **133** (2009), 445–452.
- [LiMa] F. Martin, J. H. S. de Lira, Translating solitons in Riemannian products, *J. Differential Equations* **266** (2019), 7780–7812.
- [Lop] R. López, Invariant surfaces in Euclidean space with a log-linear density, *Adv. Math.* **339** (2018), 285–309.
- [Maz] L. Mazet, Cylindrically bounded constant mean curvature surfaces in  $\mathbb{H}^2 \times \mathbb{R}$ , *Trans. Amer. Math. Soc.* **367** (2015), no. 8, 5329–5354.
- [MePe] W. H. Meeks III, J. Pérez, Constant mean curvature surfaces in metric Lie groups. In *Geometric Analysis*, **570** 25–110. Contemporary Mathematics, 2012.
- [Min] H. Minkowski, Volumen und Oberfläche, *Math. Ann.* **57** (1903), 447–495.
- [NeRo] B. Nelli and H. Rosenberg, Simply connected constant mean curvature surfaces in  $\mathbb{H}^2 \times \mathbb{R}$ . *Michigan Math. J.* **54** (2006), 537–543.
- [PeRi] R. H. L. Pedrosa, M. Ritoré, Isoperimetric domains in the Riemannian product of a circle with a simply connected space form and applications to free boundary problems. *Indiana Univ. Math. J.* **48** (1999), 1357–1394.
- [Pog] A.V. Pogorelov, Extension of a general uniqueness theorem of A.D. Aleksandrov to the case of nonanalytic surfaces (in Russian), *Doklady Akad. Nauk SSSR* **62** (1948), 297–299.